

# A Multi-Stage Hybrid CNN-Transformer Network for Automated Pediatric Lung Sound Classification

Samiul Based Shuvo<sup>1</sup>, Taufiq Hasan<sup>1,\*</sup>, *Member, IEEE*

**Abstract**—Automated analysis of lung sound auscultation is essential for monitoring respiratory health, especially in regions facing a shortage of skilled healthcare workers. While respiratory sound classification has been widely studied in adults, its application in pediatric populations, particularly in children aged <6 years, remains an underexplored area. The developmental changes in pediatric lungs considerably alter the acoustic properties of respiratory sounds, necessitating specialized classification approaches tailored to this age group. To address this, we propose a multistage hybrid CNN-Transformer framework that combines CNN-extracted features with an attention-based architecture to classify pediatric respiratory diseases using scalogram images from both full recordings and individual breath events. Our model achieved an overall score of 0.9039 in binary event classification and 0.8448 in multiclass event classification by employing class-wise focal loss to address data imbalance. At the recording level, the model attained scores of 0.720 for ternary and 0.571 for multiclass classification. These scores outperform the previous best models by 3.81% and 5.94%, respectively. This approach offers a promising solution for scalable pediatric respiratory disease diagnosis, especially in resource-limited settings.

**Index Terms**—Lung auscultation sound, respiratory disease detection, transformer, continuous wavelet transform, scalogram, focal Loss.

## I. INTRODUCTION

The respiratory system plays a pivotal role in human health, making it crucial to accurately diagnose respiratory diseases (RDs) and monitor patient conditions. Common RDs include asthma, chronic obstructive pulmonary disease (COPD), pneumonia, and bronchitis, which are the third leading cause of death in the world [1]. Early diagnosis of RDs is crucial for effective treatment and improving patient survival rates. In clinical medicine, lung auscultation has long served as a foundational method for the assessment of respiratory health. It is typically the first diagnostic step performed by healthcare professionals when evaluating patients with respiratory complaints due to its simplicity, non-invasiveness, and cost-effectiveness. Using a stethoscope, clinicians can detect and interpret a wide range of adventitious respiratory sounds (ARS), such as wheezes, crackles, rhonchi, and stridor, which often serve as early indicators of respiratory disorders [2], [3]. These sounds reflect underlying pathophysiological changes in airflow, secretion dynamics, or airway obstruction and can guide timely clinical decisions even before more advanced diagnostic tools are employed.

Despite its convenience, traditional auscultation has significant limitations. The diagnostic outcome is highly dependent

on the level of experience of the clinician, auditory sensitivity, and training. Furthermore, external noise, patient variability, and subtle acoustic differences often contribute to inter-observer inconsistency, making it challenging to standardize auscultation across practitioners and healthcare settings. In resource-limited environments where access to specialized care and advanced imaging is constrained, this variability further compounds diagnostic uncertainty [4], [5]. To address these challenges, the integration of electronic stethoscopes with artificial intelligence (AI)-based analysis systems has garnered increasing attention. Electronic stethoscopes allow for high-fidelity, noise-reduced recording of lung sounds, and can store, transmit, and replay auscultation data. When paired with AI algorithms these systems can extract robust features from lung sound signals, enabling automatic detection and classification of pathological events with high accuracy and consistency [6]. Unlike traditional auscultation, AI-driven systems are not limited by human perceptual boundaries, and offer scalable, repeatable, and objective assessments that reduce the reliance on specialist interpretation. These technologies hold substantial promise for improving respiratory care, particularly in rural clinics, emergency diagnosis settings, and telehealth platforms where rapid decision making and limited expert availability are key constraints. In addition, AI-augmented auscultation systems can serve as helper tools for medical training and second opinion generation, supporting clinical decision-making even in well-funded environments. The convergence of portable auscultation hardware and intelligent diagnostic algorithms thus marks a significant step toward democratizing respiratory health assessment and achieving more equitable healthcare outcomes globally.

Currently, there are two main types of AI-based solutions for the classification and detection of lung anomalies from sound. Earlier approaches primarily relied on feature engineering methods, where handcrafted feature sets such as Mel-frequency cepstral coefficients (MFCCs) [17], wavelet transforms (WT) [18], and short-time Fourier transform (STFT) spectrograms [19] were extracted and fed into machine learning classifiers. Traditional models such as Hidden Markov Models (HMMs) [20], Support Vector Machines (SVMs) [21], and Decision Trees [22] were widely used for classifying adventitious respiratory sounds, including wheezes, crackles, and rhonchi using these features. While these approaches achieved reasonable performance, their reliance on handcrafted feature extraction methods limited their adaptability. A more recent group of studies has focused on transforming audio recordings into two-dimensional representations while employing deep learning techniques. These data-driven deep

\*Corresponding author

<sup>1</sup>Samiul Based Shuvo, and Taufiq Hasan are with Department of Biomedical Engineering, BUET, Email: sbshuvo@bme.buet.ac.bd,taufiq@bme.buet.ac.bd.

TABLE I  
SUMMARY OF THE RECENT DEEP LEARNING-BASED WORKS ON LUNG SOUND CLASSIFICATION

Study	DL Technique	Input Features	Disease Classification	Performance Metrics
Dokur et al. [7] (2003)	MLP	MFCC, Spectrogram	COPD	Precision: 0.90, Recall: 0.85
Nishi et al. [8] (2019)	SVM, KNN, DT	Lung sound & spirometry features	COPD	Acc. 83.6%
Acharya et al. [9] (2020)	CNN-LSTM	Mel-spectrograms	Breathing cycles	ICBHI score 66.31%
Shuvo et al. [10] (2020)	Lightweight CNN	Scalograms	Pathological Condition	ICBHI score 98.70% (6-class)
Basu et al. [11] (2020)	GRU	MFCC	Pathological	Acc.: 95.25%
Nguyen et al. [12] (2020)	CNN Snapshot Ensemble	Mel-spectrogram	Breathing cycles	Acc.: 78.4% (4-class), 83.7% (2-class)
Sudha et al. [13] (2021)	Transfer learning	Scalogram	Breathing cycles	Acc.: 92.50% (ICBHI) & 92.68% (RALE)
Tariq et al. [14] (2022)	DCNN	Spectrogram, MFCC, Chromagram	Pathological Condition	Acc. 99.1%
Brunese et al. [15] (2022)	ANN	Statistical Feature Set	Pathological Condition	Acc. 98.0%
Semmad et al. [16] (2023)	CNN	Mel-spectrogram	Respiratory disorders	Acc. 98.5%

learning approaches eliminate the need for manual feature selection [10], [23]–[26]. For instance, convolutional Neural Networks (CNNs) [23], [24] with spectrogram-based representations of respiratory sounds enable automated learning of relevant audio patterns. In contrast, recurring neural networks (RNNs) and attention mechanisms have been used to capture long-term temporal dependencies in respiratory signals, further improving the classification accuracy [25], [26]. In [10], lightweight architectures based on hybrid scalograms have demonstrated promising results in detecting abnormal respiratory sound events. A short summary of deep learning-based work on respiratory sound classification is provided in Table I.

The pediatric population is affected by a variety of respiratory conditions, with pediatric pneumonia remaining a particularly critical public health concern. It accounts for a substantial proportion of hospitalizations and mortality in children under five [27], [28]. Despite the severity of these conditions, the development of automated respiratory sound classification systems has primarily focused on adult populations. A major limiting factor has been the lack of publicly available datasets representative of younger age groups. The recent release of the SPRSound dataset [29], specifically curated for pediatric patients, represents a significant milestone in this domain. ResNet [30], [31], Inception [32], [33], DL+ML [34] based, architectures have been utilized to process spectrogram-based representations of pediatric respiratory sounds, allowing for automated learning of relevant audio patterns. The combination of Inception and ResNet architectures proposed by Ngo et al. [33] captures features at multiple scales, while ResNet provides residual connections to ease the training of deeper networks. This hybrid architecture allows the model to learn richer features from spectrograms, making it particularly well-suited for classifying complex respiratory sounds. To further improve model performance, Ngo et al. [32] proposed incorporating multi-head attention mechanisms. This technique allows the model to focus on different spectral and temporal features across multiple spectrograms simultane-

ously. The attention mechanism helps the model to prioritize the most informative parts of the lung sounds, improving the accuracy of classification, especially for subtle anomalies in the sounds. Li et al. [31] introduced Focal Loss, which helps improve the recall of these minority classes, making the classification model more robust in identifying rare but clinically important respiratory events. A key challenge in this dataset is class imbalance, where normal respiratory sounds are overrepresented compared to adventitious sounds. This imbalance skews the predictions of the model, reducing the sensitivity to abnormal cases. Various strategies have been proposed to address this problem, including data enhancement techniques such as MixUp [35], SMOTE technique [36]. More recently, contrastive learning techniques have been introduced to enhance feature representation by clustering similar respiratory events [37].

Despite notable advancements in pediatric respiratory sound classification, most existing approaches predominantly concentrate on cycle-level classification, where each respiratory cycle is independently analyzed. While this granularity can aid in capturing local pathological patterns, it often overlooks the broader temporal dependencies and contextual information present across entire recordings. Consequently, such models struggle with real-world applicability, where clinical decisions typically rely on interpreting the overall respiratory pattern over extended periods, rather than isolated events. These limitations underscore the need for a more comprehensive framework that not only excels in identifying pathological events at a fine-grained level but also aggregates and contextualizes these events to make reliable recording-level decisions. Addressing these challenges, this work introduces a novel multi-stage hybrid model that couples efficient feature extraction with sophisticated feature-emphasizing and aggregation strategies to bridge the gap between event-level precision and recording-level reliability. A beifr overview of the study is illustrated in Figure 1.

The major contributions of this work are outlined as follows:

- Proposed a multi-stage hybrid model that integrates the

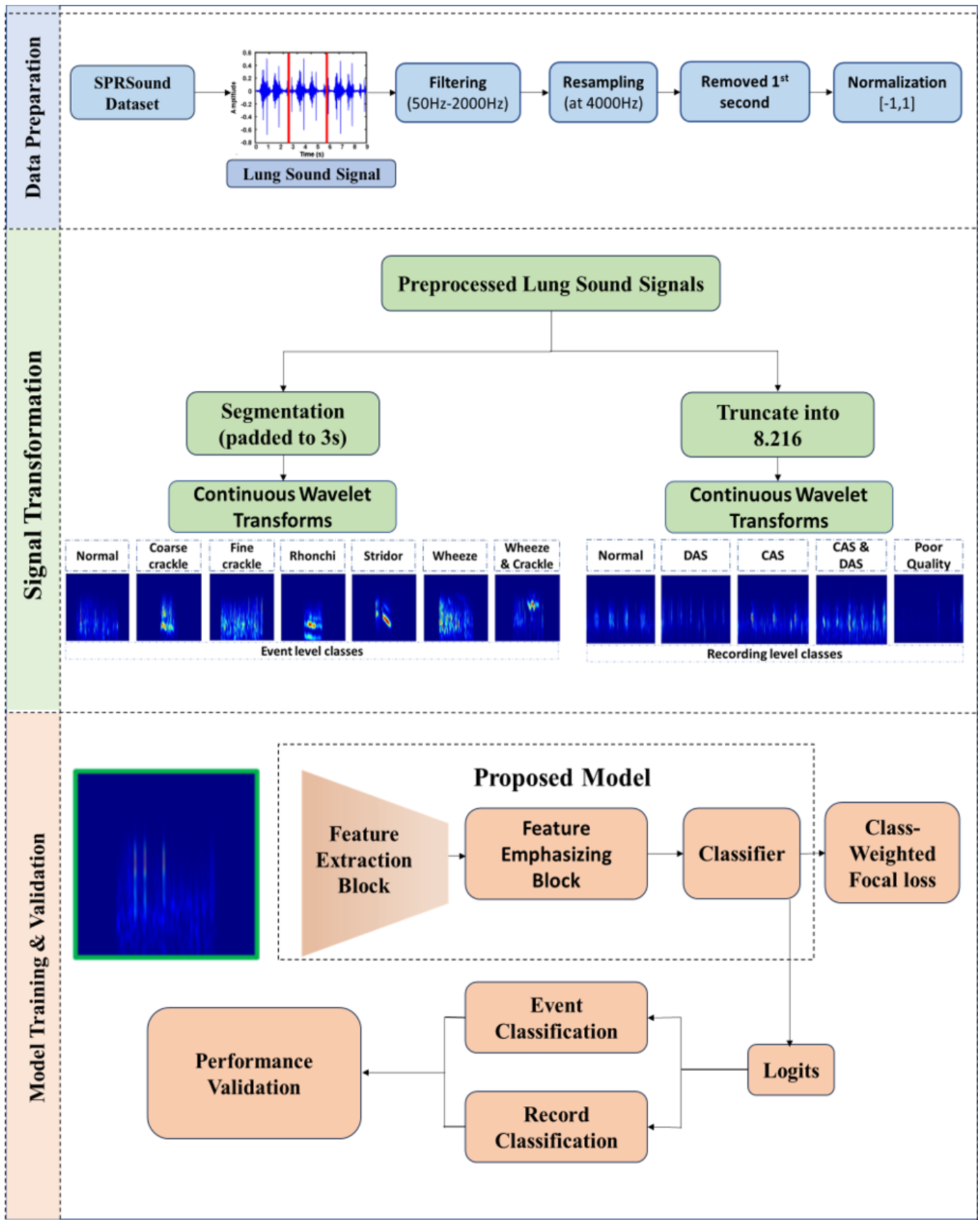


Fig. 1. A graphical overview of the proposed framework for lung sound analysis. The framework begins with the SPRsound dataset, followed by several pre-processing steps, including low-pass filtering, resampling, and normalization. The lung sound signals are then segmented based on labels and padded to a fixed length. These transformed signals are then fed into the proposed model, which performs classification tasks, including (i) normal vs. adventitious sounds (CAS, DAS) and (ii) categorization into specific respiratory sound events such as wheeze, crackle, and rhonchi.

efficiency of MobileNetV2 for feature extraction with the Transformer-based self-attention mechanisms for feature emphasizing, which improves the classification of pediatric respiratory sounds.

- Incorporated a class-weighted sparse categorical focal loss, which gives lower weights to easily classified examples and focuses on harder-to-classify cases, mitigating the class imbalance present in respiratory sound datasets.
- Conducted extensive experiments and compared the performance of the proposed model against existing state-of-the-art systems, demonstrating superior accuracy and robustness, especially in the classification of both cycle-level and recording-level tasks.
- Conducted experiments to demonstrate how the feature emphasizing block enhances the model’s ability to differentiate between respiratory sound classes, improving interpretability and decision-making.

The rest of the paper is organized as follows. Section II provides an overview of the data resources, the pre-processing methods and the feature extraction method, followed by the description of the proposed novel architecture in Section III. Section IV outlines the experimental setup, and the results are presented and discussed in Section V. Finally, the limitations and future scope of the work are presented in Section VI, followed by the conclusion in Section VII.

## II. MATERIALS AND METHODS

### A. Dataset

In this study, we utilized the open-access SPRSound pediatric respiratory sound database developed by Shanghai Jiao Tong University [29]. The dataset has been used for the IEEE BioCAS 2022 challenge. This database is the first open-access pediatric respiratory sound database, addressing a gap in existing datasets that predominantly focus on adult populations. This database consists of 2,683 records and 9,089 respiratory sound events from 292 participants [29]. The database categorizes the data at two levels: Record Level (represents the classification of the entire respiratory sound record) and Event Level (individual respiratory sound events within the recordings). A detailed class distribution is shown in Table II.

### B. Data Pre-processing

1) *Bandpass filtering*: Lung auscultation signals typically fall within the frequency range of 50 to 2000 Hz [38]. To pre-process the audio samples of lung sound, a 4th-order Butterworth bandpass filter is applied, with the lower and upper cutoff frequencies set at 50 Hz and 2000 Hz, respectively. In order to maintain consistency and preserve key lung sound features while minimizing computational load, all audio samples are resampled at a frequency of 4 kHz. In addition, the signals are normalized in amplitude to mitigate the variations caused by different devices or sensors.

2) *Segmentation*: The dataset primarily contains audio samples of two durations: 9.216 seconds (1924 samples) and 15.216 seconds (759 samples). To pre-process the data, the

TABLE II  
SPRSOUND DATASET CLASS DISTRIBUTION FOR TRAINING AND TESTING

Level	Type	Training	Testing
Record	Normal	1303	482
	Continuous adventitious sounds (CAS)	126	107
	Discontinuous adventitious sounds (DAS)	248	99
	CAS & DAS	95	36
	Poor Quality	177	10
	<b>Total</b>	<b>1,949</b>	<b>734</b>
Event	Normal	5159	1728
	Rhonchi	39	14
	Wheeze	452	413
	Stridor	15	2
	Coarse Crackle	49	17
	Fine Crackle	912	255
	Wheeze & Crackle	30	4
	<b>Total</b>	<b>6,656</b>	<b>2,433</b>

first second of each recording is removed to eliminate the initial friction sound from the stethoscope. After this, the remaining 8.216-second segment is used for analysis. For the 15.216-second samples, we select either the first 8.216 seconds (0–8.216) or the last 8.216 seconds (7–15.216), depending on which segment contains more respiratory events. At the event level, each lung sound recording is segmented according to the timing of the annotated respiratory cycles. The cycle samples are then transformed into homogeneous signals with a fixed duration of 3 seconds with zero padding [39].

### C. Transformation into 2D images

The Continuous Wavelet Transform (CWT) is a signal processing technique that allows the decomposition of a signal into an orthonormal wavelet basis or a set of independent frequency components [40], [41]. By using a basis function, i.e. the mother wavelet  $g(t)$ , and it is scaled and shifted versions, the CWT can decompose a finite-energy signal  $x(t)$  as follows [42]:

$$Z(a, b) = \frac{1}{\sqrt{b}} \int x(t) g\left(\frac{t-a}{b}\right) dt \quad (1)$$

Here,  $a$  and  $b$  represent the scale and translation parameters, respectively. The squared magnitude of the CWT coefficients  $Z$  is referred to as the scalogram [40]. Both the 8.216-second (recorded) and 3-second (segmented) lung sound samples are analyzed in the wavelet domain using the Morse analytic wavelet as the mother wavelet, and the scalogram images of  $224 \times 224$  resolution are produced. The time-bandwidth product and symmetry parameter for the wavelet are set to 60 and 3, respectively. The range of energy for the wavelet in both time and frequency determines the minimum and maximum scales, which are automatically chosen using 10 voices per octave [43].

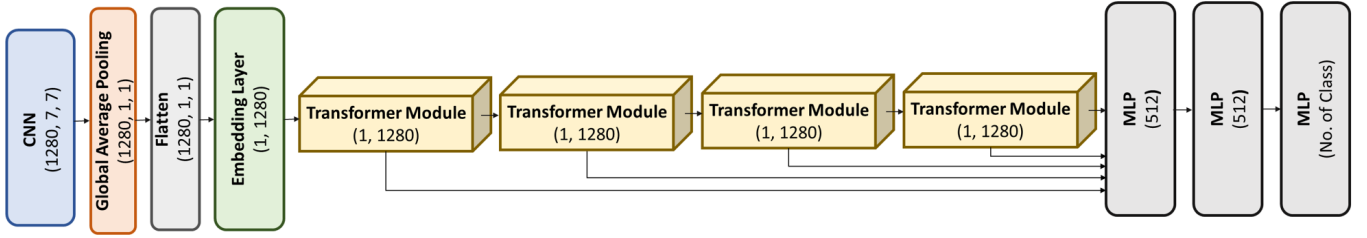


Fig. 2. Architecture of the proposed Multi-Stage Hybrid CNN-Transformer model for respiratory sound classification. The model consists of a MobileNet feature extractor, followed by global average pooling, an embedding layer, and a series of Transformer modules ( 8 attention heads with a hidden size of 2048). The final classification is performed by a multi-layer perceptron (MLP) to predict the diagnostic classes.

### III. PROPOSED CLASSIFIER ARCHITECTURE

The proposed model is designed for the classification of lung sound scalograms. This architecture effectively combines a lightweight convolutional feature extraction network (with the network selection process described in Section V-A), self-attention-based feature refinement, and a robust classifier to achieve efficient and accurate respiratory sound classification. The integration of depthwise separable convolutions and transformer-based attention enables the model to process spectro-temporal lung sound representations with improved generalization and computational efficiency. The overall architecture is illustrated in Figure 2.

#### A. Feature Extraction Block

The feature extraction block utilizes MobileNetV2 [44], a lightweight CNN optimized for efficient feature extraction. MobileNetV2 employs depthwise separable convolutions, significantly reducing computational complexity while retaining rich feature representations. The input to the model consists of 2D scalogram representations of lung sound signals with dimensions  $224 \times 224 \times 3$ . The first convolutional layer applies a  $3 \times 3$  kernel with 32 filters, followed by a series of inverted residual blocks with linear bottlenecks to enhance feature expressiveness. The depthwise separable convolution is mathematically formulated as follows:

$$Y = (X * D) * P \quad (2)$$

where:

- $X$  represents the input feature map,
- $D$  is the depthwise convolution kernel,
- $P$  is the pointwise convolution kernel,
- $*$  denotes the convolution operation.

This operation significantly reduces the number of parameters compared to standard convolutions. The final output from MobileNetV2 is a feature map of size  $7 \times 7 \times 1280$ , which is further refined in the next stage.

#### B. Feature Emphasizing Block

To enhance the extracted feature representations, the model incorporates a transformer-based self-attention mechanism. Unlike traditional CNNs, which rely on local spatial hierarchies, the transformer module captures global contextual dependencies across temporal and spectral dimensions [45].

The feature maps from MobileNetV2 are first flattened and projected into a 1280-dimensional embedding space, which serves as the input to the multi-head self-attention module.

The self-attention mechanism is mathematically formulated as follows:

$$\text{Attention}(Q, K, V) = \text{softmax}\left(\frac{QK^T}{\sqrt{d_k}}\right)V \quad (3)$$

Where:

- $Q, K, V$  are the query, key, and value matrices,
- $d_k$  is the dimensionality of the key vectors,

Our model employs eight attention heads, each computing an independent attention score, followed by a feedforward network with a hidden size of 2048, given by

$$\text{FFN}(x) = \max(0, xW_1 + b_1)W_2 + b_2 \quad (4)$$

where  $W_1, W_2$  and  $b_1, b_2$  are learnable parameters. Layer normalization is applied for stable training, and dropout is used to prevent overfitting. Four such transformer modules in series constitute the feature emphasizing block.

#### C. Classifier

The refined feature representations from the transformer modules are passed through the classifier, which consists of three fully connected layers. The first two fully connected layers have 512 and 256 neurons, respectively, sandwiched by a dropout layer with probability  $p = 0.3$ . The final classification layer consists of  $C$  output neurons corresponding to the number of target classes and applies the softmax activation function to compute class probabilities:

$$P(y_i) = \frac{e^{z_i}}{\sum_{j=1}^C e^{z_j}} \quad (5)$$

where,  $z_i$  is the logit for class  $i$ ,  $C$  is the total number of classes and  $P(y_i)$  represents the probability of class  $i$ .

The entire model is trained using the class-weighted sparse categorical focal loss function.

## IV. EXPERIMENTAL SETUP

### A. Task Definitions

The IEEE BioCAS 2022 challenge introduces two main tasks [29]. In this study, we opted for these tasks. Task 1, which focuses on the classification of sound events, is

divided into two subtasks: Task 1-1 and Task 1-2. Task 1-1 is responsible for categorizing respiratory sound events as either Normal or Adventitious. Task 1-2, on the other hand, further classifies these events into more specific categories, including Normal, Rhonchi (Rho), Wheeze (W), Stridor (Str), Coarse Crackle (CC), Fine Crackle (FC), and Wheeze and Crackle (WC). Task 2, which addresses the classification of the entire respiratory recording, consists of Task 2-1 and Task 2-2. Task 2-1 focuses on classifying the recording as Normal, Adventitious, or Poor Quality (PQ). Task 2-2 is a multi-class classification task, where recordings are classified into categories such as Normal, CAS (Continuous Adventitious Sounds), DAS (Discontinuous Adventitious Sounds), CAS & DAS, or PQ.

### B. Evaluation Criteria

The training audio files (both for recording level and event level classification) are split into two sets with an approximate proportion of 90 : 10 split for creating training and validation sets. The provided testing set defined by the challenge was used to evaluate the model.

To align with the evaluation metrics of the IEEE BioCAS 2022 challenge, the tasks and sub-tasks in this study are evaluated based on the following metrics: sensitivity (SE), specificity (SP), average sensitivity (AS), harmonic sensitivity (HS), and the overall score. These metrics are calculated as follows:

$$SE = \frac{T_i}{\sum N_i} \text{ and } SP = \frac{T_N}{N_N} \quad (6)$$

where  $T_i$  denotes the number of correctly classified samples of class  $i$ ,  $\sum N_i$  is the total number of samples of target class  $i$ . Similarly,  $T_N$  and  $N_N$  represent the number of correctly classified normal samples and the total number of standard samples, respectively.

Next, the average score (AS), harmonic score (HS), and the overall score (Score) are computed as follows:

$$AS = \frac{SE + SP}{2} \quad (7)$$

$$HS = \frac{2 \times SE \times SP}{SE + SP} \quad (8)$$

$$Score = \frac{AS + HS}{2} \quad (9)$$

### C. Hyperparameters

The proposed model is constructed using TensorFlow backend and trained using NVidia K80 GPUs. In this study, a batch size of 128 has been selected for all the Tasks. Optimization is performed using the Adam optimizer with a learning rate of 0.001.

TABLE III  
PERFORMANCE COMPARISON OF DIFFERENT FEATURE EXTRACTOR MODELS FOR RECORDING-LEVEL AND CYCLE-LEVEL CLASSIFICATION TASKS

Cycle level Classification										
	Task 1-1					Task 1-2				
	SE	SP	AS	HS	Score	SE	SP	AS	HS	Score
<b>MobileNetV2</b>	<b>0.85</b>	<b>0.89</b>	<b>0.86</b>	<b>0.86</b>	<b>0.86</b>	<b>0.75</b>	<b>0.88</b>	<b>0.82</b>	<b>0.81</b>	<b>0.815</b>
<b>Inception V2</b>	0.83	0.87	0.85	0.84	0.845	0.73	0.86	0.78	0.77	0.775
<b>ResNetV2</b>	0.81	0.86	0.79	0.78	0.785	0.74	0.87	0.80	0.79	0.795
<b>VGG 16</b>	0.78	0.84	0.81	0.80	0.805	0.72	0.85	0.77	0.76	0.765
Recording level Classification										
	Task 2-1					Task 2-2				
	SE	SP	AS	HS	Score	SE	SP	AS	HS	Score
<b>MobileNetV2</b>	<b>0.710</b>	0.675	<b>0.690</b>	<b>0.685</b>	<b>0.688</b>	0.425	0.701	0.563	0.529	0.546
<b>Inception V2</b>	0.695	<b>0.690</b>	0.680	0.675	0.678	0.460	0.725	0.590	0.560	0.575
<b>ResNetV2</b>	0.685	0.680	0.670	0.660	0.665	<b>0.480</b>	<b>0.740</b>	<b>0.605</b>	<b>0.570</b>	<b>0.590</b>
<b>VGG16</b>	0.670	0.665	0.660	0.650	0.655	0.435	0.710	0.570	0.540	0.555

### D. Loss Function

To enhance the detection of rare classes of lung sounds while solving the class imbalance problem, we employed a class-weighted sparse categorical focal loss function. This loss function incorporates a focusing parameter  $\gamma$  that guides the function to focus on complex examples more than easily classified examples, thereby improving model robustness to hard-to-classify cases [46]. The focal loss is defined as follows:

$$L(y, \hat{\mathbf{p}}) = -w_y(1 - \hat{p}_y)^\gamma \log(\hat{p}_y) \quad (10)$$

Where:

- $y \in \{0, \dots, K-1\}$  represents the ground truth class label for  $K$  classes,
- $\hat{\mathbf{p}} = [\hat{p}_0, \hat{p}_1, \dots, \hat{p}_{K-1}]$  represents the predicted probability distribution over  $k$  classes,
- $\gamma$  is the **focusing parameter**, which down-weights easy examples and emphasizes harder cases,
- $w_y$  is the class-specific weight used to counteract the class imbalance.

## V. RESULTS AND DISCUSSION

### A. Selection of the Feature Extractor Model

We experiment with four state-of-the-art models (MobileNetV2 [44], Inception-V2 [47], ResNetV2 [48], and VGG16 [49]) to determine which model works best as the feature extractor in our model. These models were tested across both cycle-level and recording-level classification (as shown in the Table III).

In cycle-level classification, MobileNetV2 shows the highest scores in both tasks, achieving a score of 0.815 in Task 1-2, with high sensitivity and specificity values. Similarly, in the recording level performance, MobileNetV2 achieved the best overall balance in terms of sensitivity and specificity. In Task 2-1, it showed strong performance with a score of 0.675 for sensitivity and 0.710 for specificity. This indicates that MobileNetV2 is effective at detecting relevant features in the data while keeping errors to a minimum. Although

TABLE IV  
PERFORMANCE COMPARISON OF PROPOSED MODEL AT DIFFERENT  $\gamma$  VALUES FOR CYCLE AND RECORDING-LEVEL CLASSIFICATION

Cycle-Level Classification										
	Task 1-1					Task 1-2				
	SE	SP	AS	HS	Score	SE	SP	AS	HS	Score
$\gamma = 2$	0.891	0.910	0.900	0.900	0.900	0.765	0.909	0.837	0.831	0.838
$\gamma = 3$	0.895	0.905	0.900	0.900	0.900	0.753	<b>0.931</b>	0.842	0.833	0.838
$\gamma = 4$	0.891	<b>0.914</b>	<b>0.904</b>	<b>0.904</b>	<b>0.904</b>	<b>0.783</b>	0.912	<b>0.847</b>	<b>0.842</b>	<b>0.845</b>
$\gamma = 5$	<b>0.903</b>	0.905	0.902	0.902	0.900	0.769	0.901	0.839	0.830	0.832
Recording-Level Classification										
	Task 2-1					Task 2-2				
	SE	SP	AS	HS	Score	SE	SP	AS	HS	Score
$\gamma = 2$	<b>0.726</b>	0.670	0.697	0.696	0.696	<b>0.446</b>	0.716	0.581	0.550	0.566
$\gamma = 3$	0.612	<b>0.807</b>	0.709	0.698	0.706	0.418	<b>0.780</b>	<b>0.599</b>	<b>0.544</b>	<b>0.571</b>
$\gamma = 4$	0.665	0.718	0.692	0.691	0.691	0.397	0.757	0.577	0.526	0.549
$\gamma = 5$	0.590	0.843	<b>0.730</b>	<b>0.710</b>	<b>0.720</b>	0.434	0.734	0.584	0.546	0.565

MobileNetV2 had a slightly lower score of 0.546 compared to other models in Task 2-2, it still performed fairly well in comparison. This consistent performance across both tasks highlighted its robustness and versatility with relatively low computational cost. Therefore, we chose MobileNetV2 as the feature extractor for our model.

### B. Ablation Study

To evaluate the impact of the focal loss parameter  $\gamma$  on classification performance, we conducted an ablation study across different  $\gamma$  values ranging from 2 to 5. This analysis helps isolate and understand the role of  $\gamma$  in tuning the loss function's focus on hard-to-classify examples and providing insights into its influence across tasks of varying granularity. The results, detailed in Table IV, highlight the sensitivity of both cycle-level and recording-level classification tasks to this hyperparameter.

In the cycle-level classification task, our model demonstrated promising results in distinguishing between different respiratory sounds' characteristics across both Task 1-1 and Task 1-2 (as seen in Table IV). In Task 1-1, a  $\gamma$  value of 4 yielded the best performance, achieving a score of 0.9039, which showed a 0.41% improvement over the baseline  $\gamma = 2$  model, indicating its efficacy in capturing key features of the respiratory sounds. The improvement in performance was more noticeable in Task 1-2, where  $\gamma = 4$  again outperformed the other  $\gamma$  configurations, achieving an overall score of 0.8448, which was a 0.85% improvement over  $\gamma = 2$ . Similarly, high sensitivity and specificity values reflect the model's superior ability to generalize across various adventitious sound types.

Due to the challenges of noise and variability across entire recordings, the proposed model's results for the recording level classification task demonstrated a more varied performance across the different  $\gamma$  values (as seen in Table IV). In Task 2-1,  $\gamma = 5$  achieves the highest score of 0.720, with a significant specificity gain (SP = 0.843, highest among all models), indicating its strong ability to reduce false positives.

TABLE V  
PERFORMANCE COMPARISON OF PROPOSED MODEL WITH DIFFERENT SOTA MODELS FOR CYCLE AND RECORDING-LEVEL CLASSIFICATION

Cycle level Classification										
	task 1-1					Task 1-2				
	SE	SP	AS	HS	Score	SE	SP	AS	HS	Score
Ngo et al. [32]	0.810	0.910	0.860	0.860	0.860	0.670	0.920	0.790	0.780	0.790
Pham et al. [33]	0.840	0.855	0.849	0.849	0.849	0.678	0.883	0.781	0.767	0.774
Moummad et al. [37]	0.890	0.900	0.890	0.890	0.890	0.680	<b>0.940</b>	0.810	0.790	0.800
Chen et al. [30]	0.890	0.900	0.890	0.890	0.890	0.680	<b>0.940</b>	0.810	0.790	0.800
Proposed Model	<b>0.891</b>	<b>0.914</b>	<b>0.904</b>	<b>0.904</b>	<b>0.904</b>	<b>0.783</b>	0.912	<b>0.847</b>	<b>0.842</b>	<b>0.845</b>
Recording level Classification										
	Task 2-1					Task 2-2				
	SE	SP	AS	HS	Score	SE	SP	AS	HS	Score
Ngo [32]	0.670	0.760	0.710	0.710	0.710	0.400	0.760	0.520	0.520	0.550
Pham et al. [33]	0.704	0.789	<b>0.747</b>	<b>0.744</b>	<b>0.745</b>	0.361	0.801	0.581	0.498	0.539
Moummad et al. [37]	<b>0.770</b>	0.660	0.720	0.710	0.715	0.230	<b>0.860</b>	0.540	0.360	0.450
Chen et al. [30]	0.770	0.660	0.720	0.710	0.710	0.230	0.860	0.540	0.360	0.450
Proposed Model	0.612	<b>0.807</b>	0.709	0.698	0.706	<b>0.418</b>	0.780	<b>0.599</b>	<b>0.544</b>	<b>0.571</b>

However, in Task 2-2,  $\gamma = 3$  outperforms others with a score of 0.571, showing a 0.89% improvement over the baseline  $\gamma = 2$  (0.566) configuration.

The performance gap between cycle-level and recording-level tasks is evident, with cycle-level accuracy surpassing recording-level accuracy by 9–15%, highlighting the difficulty of handling extended respiratory segments. Here, we chose  $\gamma = 4$  and  $\gamma = 3$  as optimal values of our proposed model for cycle-level and recording-level classification, respectively,

### C. Comparison with Existing Methods

In this study, our proposed model is compared with existing state-of-the-art methods in the classification of respiratory sounds. Table V presents a summary of this comparative analysis, highlighting key performance metrics in different classification tasks at the cycle and record levels.

Chen et al. [30] employed a fine-tuned ResNet18 architecture utilizing STFT spectrogram features, achieving notable scores, particularly on Tasks 1-1 and 1-2. However, their method exhibits limitations in generalization, as evidenced by relatively lower scores in Tasks 2-1 and 2-2 (0.710 and 0.450, respectively). Moummad et al. [37] explored supervised contrastive learning that incorporates demographic metadata, improving generalization and anomaly detection. Despite demonstrating effective performance across multiple datasets, their approach still struggles with computational inefficiency and complexity arising from additional metadata dependencies, resulting in moderate scores (0.715 in Task 2-1 and 0.450 in Task 2-2). In contrast, our proposed method consistently demonstrates superior performance across both cycle and recording-level classifications. It achieves exceptional robustness and generalization, particularly evidenced by a superior overall Score of 0.904 in Task 1-1 and 0.845 in Task 1-2 also 0.720 and 0.571 in Task 2-1 and 2-2, respectively, significantly surpassing Chen et al. and Moummad et al. Although methods like those proposed by [32] and [33] are effective in controlled environments, they struggle with noise and environmental artifacts in clinical recordings. In Task 2-2, their results struggle to maintain accuracy in the presence

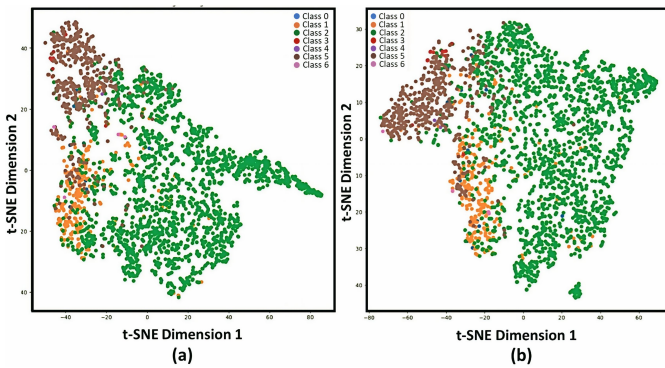


Fig. 3. Two t-SNE plots of feature embeddings : one representing the MobileNetV2 model (left) and the other our proposed model (right) with incorporated feature emphasizing through transformer blocks

of background noise variations in respiratory sound patterns, leading to unreliable predictions in noisy settings. However, our proposed method consistently demonstrates a 3.81% and 5.94% performance gain, respectively.

#### D. Effect of Feature Enhancement on Embedding Space Separation

In this study, we found that introducing a feature-enhancing block enhances the feature extraction process with MobileNetV2. To effectively analyze this, we compared two t-SNE (t-Distributed Stochastic Neighbor Embedding) plots of feature embeddings: one representing the MobileNetV2 model (left) and the other our proposed model (right) with incorporated feature emphasizing through transformer blocks (shown in Figure 3).

t-SNE plot works by mapping high-dimensional data points to a lower-dimensional space (typically 2D or 3D) while attempting to preserve the pairwise similarities between data points. Figure 3 (a) demonstrated the t-SNE visualization for the MobileNetV2 model without feature emphasizing, highlighting its limitations in class separation. A significant overlap between multiple classes, particularly Class 0 (green) and Class 3 (red) and Class 4 (orange) and Class 5 (purple), have been observed in this plot. The clustering of these classes suggests that the model has difficulty learning discriminative features and fails to separate these classes in the higher-dimensional space. In contrast, the proposed model demonstrated a much more apparent separation between the classes (shown in Figure 3 (b)). Here, Class 0 (green) is now well-separated from Class 3 (red), and Class 2 (yellow) is clearly distinguished from Class 5 (purple). This enhanced separation in the t-SNE plot indicates that the feature-emphasizing mechanism helps the model to focus on the most discriminative features, improving the clarity of class boundaries and enhancing overall model performance in higher-dimensional space.

#### VI. LIMITATION AND FUTURE WORK

While the proposed framework demonstrates promising results, its interpretability remains a significant concern for

clinical deployment. The lack of transparency in decision-making processes can hinder clinicians' trust and limit real-world integration. Enhancing explainability through interpretable machine learning techniques and visualization tools is essential to support clinical validation and user acceptance. Moreover, further optimization is necessary to enable real-time performance, especially in resource-constrained or point-of-care settings, where latency and computational efficiency are critical. Additionally, the current classification model has been trained on specific datasets, which may not comprehensively capture the diversity of respiratory conditions across different populations, age groups, and clinical scenarios. The limited availability of large-scale, well-annotated, and standardized datasets continues to be a major bottleneck in developing robust and generalizable models.

Future research directions should explore the development of more sophisticated and context-aware frameworks that integrate a patient's clinical history, presenting symptoms, and anatomical characteristics along with radiological image findings. Such holistic approaches can improve diagnostic accuracy and personalize treatment strategies. Moreover, there are scopes for analyzing other multimodal approaches using different types of physiological signals and imaging modalities.

#### VII. CONCLUSION

This study addressed the precise classification of pediatric respiratory diseases at both the event and recording levels. For that, we proposed a multi-stage hybrid CNN-Transformer model for classifying lung sounds, which effectively combines MobileNet-V2 for efficient feature extraction with transformer-based self-attention for enhanced feature refinement. The model demonstrated superior performance across event-level and recording-level tasks and has achieved a significantly high overall score of 0.9039 and 0.8448 for Task 1-1 and Task 1-2, respectively, in breath event classification. Similarly, the model outperformed all the SOTA systems at Task 2-2 with a score of 0.5710. However, the model has limitations, including reliance on a relatively small dataset and high computational demands.

#### REFERENCES

- [1] I. Newsroom, "Chronic respiratory disease is third leading cause of death globally with air pollution killing 1.3 million people," IHME Newsroom, 4 2023, accessed: 2023-12-14. [Online]. Available: <https://www.healthdata.org/news-events/newsroom/news-releases/chronic-respiratory-disease-third-leading-cause-death-globally>
- [2] S. Reichert, R. Gass, C. Brandt, and E. Andr s, "Analysis of respiratory sounds: state of the art," *Clin. Med. Circ. Respirat. Pulm. Med.*, vol. 2, pp. CCRPM-S530, 2008.
- [3] A. Bohadana, G. Izbicki, and S. S. Kraman, "Fundamentals of lung auscultation," *N. Engl. J. Med.*, vol. 370, no. 8, pp. 744-751, 2014.
- [4] A. Gurung, C. G. Scrafford, J. M. Tielsch, O. S. Levine, and W. Checkley, "Computerized lung sound analysis as diagnostic aid for the detection of abnormal lung sounds: a systematic review and meta-analysis," *Respir. Med.*, vol. 105, no. 9, pp. 1396-1403, 2011.
- [5] N. Babu, J. Kumari, J. Mathew, U. Satija, and A. Mondal, "Multiclass categorisation of respiratory sound signals using neural network," in *Proc. BioCAS*. IEEE, 2022, pp. 228-232.
- [6] A. Moberg,  . I. Emilsson, S. Hansdottir, T. Asmundsson, A. Malinovsky, H. Melbye, and D. Ludviksdottir, "Lung auscultation-today and tomorrow: a narrative review," *Expert Rev. Respir. Med.*, pp. 1-7, May 2025.

- [7] Z. Dokur and T. Ölmez, "Classification of respiratory sounds by using an artificial neural network." *Int. J. Pattern Recognit. Artif. Intell.*, vol. 17, no. 4, 2003.
- [8] N. S. Haider, B. K. Singh, R. Periyasamy, and A. K. Behera, "Respiratory sound based classification of chronic obstructive pulmonary disease: a risk stratification approach in machine learning paradigm," *J. Med. Syst.*, vol. 43, no. 8, p. 255, 2019.
- [9] J. Acharya and A. Basu, "Deep neural network for respiratory sound classification in wearable devices enabled by patient specific model tuning," *IEEE Trans. Biomed. Circuits Syst.*, vol. 14, no. 3, pp. 535–544, 2020.
- [10] S. B. Shuvo, S. N. Ali, S. I. Swapnil, T. Hasan, and M. I. H. Bhuiyan, "A lightweight cnn model for detecting respiratory diseases from lung auscultation sounds using emd-cwt-based hybrid scalogram," *IEEE J. Biomed. Health Informat.*, vol. 25, no. 7, pp. 2595–2603, 2020.
- [11] V. Basu and S. Rana, "Respiratory diseases recognition through respiratory sound with the help of deep neural network," in *Proc. CINE*. IEEE, 2020, pp. 1–6.
- [12] T. Nguyen and F. Pernkopf, "Lung sound classification using snapshot ensemble of convolutional neural networks," in *Proc. EMBC*. IEEE, 2020, pp. 760–763.
- [13] S. Jayalakshmy and G. F. Sudha, "Conditional gan based augmentation for predictive modeling of respiratory signals," *Comput. Biol. Med.*, vol. 138, p. 104930, 2021.
- [14] Z. Tariq, S. K. Shah, and Y. Lee, "Feature-based fusion using cnn for lung and heart sound classification," *Sensors*, vol. 22, no. 4, p. 1521, 2022.
- [15] L. Brunese, F. Mercaldo, A. Reginelli, and A. Santone, "A neural network-based method for respiratory sound analysis and lung disease detection," *Appl. Sci.*, vol. 12, no. 8, p. 3877, 2022.
- [16] A. Semmad and M. Bahoura, "Scalable serial hardware architecture of multilayer perceptron neural network for automatic wheezing detection," *Microprocess. Microsyst.*, vol. 99, p. 104844, 2023.
- [17] M. Bahoura and C. Pelletier, "New parameters for respiratory sound classification," in *Proc. CCECE*, vol. 3. IEEE, 2003, pp. 1457–1460.
- [18] M. Bahoura, "Pattern recognition methods applied to respiratory sounds classification into normal and wheeze classes," *Comput. Biol. Med.*, vol. 39, no. 9, pp. 824–843, 2009.
- [19] J. Acharya, A. Basu, and W. Ser, "Feature extraction techniques for low-power ambulatory wheeze detection wearables," in *Proc. EMBC*. IEEE, 2017, pp. 4574–4577.
- [20] T. Okubo, N. Nakamura, M. Yamashita, and S. Matsunaga, "Classification of healthy subjects and patients with pulmonary emphysema using continuous respiratory sounds," in *Proc. EMBC*. IEEE, 2014, pp. 70–73.
- [21] M. Grønnesby, J. C. A. Solis, E. Holsbø, H. Melbye, and L. A. Bongo, "Feature extraction for machine learning based crackle detection in lung sounds from a health survey," *arXiv preprint arXiv:1706.00005*, 2017.
- [22] G. Chambres, P. Hanna, and M. Desainte-Catherine, "Automatic detection of patient with respiratory diseases using lung sound analysis," in *Proc. CBMI*. IEEE, 2018, pp. 1–6.
- [23] L. Pham, H. Phan, R. Palaniappan, A. Mertins, and I. McLoughlin, "Cnn-moe based framework for classification of respiratory anomalies and lung disease detection," *IEEE J. Biomed. Health Informat.*, vol. 25, no. 8, pp. 2938–2947, 2021.
- [24] D. Ngo, L. Pham, A. Nguyen, B. Phan, K. Tran, and T. Nguyen, "Deep learning framework applied for predicting anomaly of respiratory sounds," in *Proc. EESYSM*. IEEE, 2021, pp. 42–47.
- [25] K. Minami, H. Lu, H. Kim, S. Mabu, Y. Hirano, and S. Kido, "Automatic classification of large-scale respiratory sound dataset based on convolutional neural network," in *Proc. ICCAS*. IEEE, 2019, pp. 804–807.
- [26] D. Perna and A. Tagarelli, "Deep auscultation: Predicting respiratory anomalies and diseases via recurrent neural networks," in *Proc. CBMS*. IEEE, 2019, pp. 50–55.
- [27] A. A. Tazinya, G. E. Halle-Ekane, L. T. Mbuagbaw, M. Abanda, J. Atashili, and M. T. Obama, "Risk factors for acute respiratory infections in children under five years attending the bamenda regional hospital in cameroon," *BMC Pulm. Med.*, vol. 18, pp. 1–8, 2018.
- [28] C. F. Lanata and R. E. Black, "Acute lower respiratory infections," in *Nutrition and Health in Developing Countries*, R. D. Semba and M. W. Bloem, Eds. Totowa, NJ: Humana Press, 2008, pp. 179–214.
- [29] Q. Zhang, J. Zhang, J. Yuan, H. Huang, Y. Zhang, B. Zhang, G. Lv, S. Lin, N. Wang, X. Liu, *et al.*, "Sprsound: Open-source sjtu paediatric respiratory sound database," *IEEE Trans. Biomed. Circuits Syst.*, vol. 16, no. 5, pp. 867–881, 2022.
- [30] Z. Chen, H. Wang, C.-H. Yeh, and X. Liu, "Classify respiratory abnormality in lung sounds using stft and a fine-tuned resnet18 network," in *Proc. BioCAS*. IEEE, 2022, pp. 233–237.
- [31] J. Li, X. Wang, X. Wang, S. Qiao, and Y. Zhou, "Improving the resnet-based respiratory sound classification systems with focal loss," in *Proc. BioCAS*. IEEE, 2022, pp. 223–227.
- [32] D. Ngo, L. Pham, H. Phan, M. Tran, and D. Jarchi, "A deep learning architecture with spatio-temporal focusing for detecting respiratory anomalies," in *Proc. BioCAS*. IEEE, 2023, pp. 1–5.
- [33] D. Ngo, L. Pham, H. Phan, M. Tran, D. Jarchi, and Ş. Kolozali, "An inception-residual-based architecture with multi-objective loss for detecting respiratory anomalies," in *Proc. MMSp*. IEEE, 2023, pp. 1–6.
- [34] B. Taghibeyglou, A. Assadi, A. Elwali, and A. Yadollahi, "Fusion of manual and deep learning analyses for automatic lung respiratory sounds identification in youth," *Proc. CMBES*, vol. 45, 2023.
- [35] J. Hu, C. S. Leow, S. Tao, W. L. Goh, and Y. Gao, "Supervised contrastive pretrained resnet with mixup to enhance respiratory sound classification on imbalanced and limited dataset," in *Proc. BioCAS*. IEEE, 2023, pp. 1–5.
- [36] L. Zhang, Y. Zhu, S. Tu, and L. Xu, "A feature polymerized based two-level ensemble model for respiratory sound classification," in *Proc. BioCAS*. IEEE, 2022, pp. 238–242.
- [37] I. Moummad and N. Farrugia, "Pretraining respiratory sound representations using metadata and contrastive learning," in *Proc. WASPAA*. IEEE, 2023, pp. 1–5.
- [38] S. Reichert, R. Gass, C. Brandt, and E. Andrès, "Analysis of respiratory sounds: state of the art," *Clin. Med. Circ. Respirat. Pulm. Med.*, vol. 2, pp. CCRPM–S530, 2008.
- [39] L. Pham, I. McLoughlin, H. Phan, M. Tran, T. Nguyen, and R. Palaniappan, "Robust deep learning framework for predicting respiratory anomalies and diseases," in *Proc. EMBS*. IEEE, 2020, pp. 164–167.
- [40] N. Gautam and S. B. Pokle, "Wavelet scalogram analysis of phonopulmonographic signals," *Int. J. Med. Eng. Inform.*, vol. 5, no. 3, pp. 245–252, 2013.
- [41] S. Debbal and F. Bereksi-Reguig, "Analysis of the second heart sound using continuous wavelet transform," *J. Med. Eng. Technol.*, vol. 28, no. 4, pp. 151–156, 2004.
- [42] A. Meintjes, A. Lowe, and M. Legget, "Fundamental heart sound classification using the continuous wavelet transform and convolutional neural networks," in *Proc. EMBS*. IEEE, 2018, pp. 409–412.
- [43] "Continuous 1-D wavelet transform - MATLAB cwt," [Online]. Available: <https://www.mathworks.com/help/wavelet/ref/cwt.html>.
- [44] A. G. Howard, M. Zhu, B. Chen, D. Kalenichenko, W. Wang, T. Weyand, M. Andreetto, and H. Adam, "Mobilenets: Efficient convolutional neural networks for mobile vision applications," *arXiv preprint arXiv:1704.04861*, 2017.
- [45] A. Vaswani, N. Shazeer, N. Parmar, J. Uszkoreit, L. Jones, A. N. Gomez, Ł. Kaiser, and I. Polosukhin, "Attention is all you need," *Adv. Neural Inf. Process. Syst.*, vol. 30, 2017.
- [46] T.-Y. Lin, P. Goyal, R. Girshick, K. He, and P. Dollár, "Focal loss for dense object detection," in *Proc. ICCV*, 2017, pp. 2980–2988.
- [47] C. Szegedy, W. Liu, Y. Jia, P. Sermanet, S. Reed, D. Anguelov, D. Erhan, V. Vanhoucke, and A. Rabinovich, "Going deeper with convolutions," in *Proc. CVPR*, 2015, pp. 1–9.
- [48] K. He, X. Zhang, S. Ren, and J. Sun, "Deep residual learning for image recognition," in *Proc. CVPR*, 2016, pp. 770–778.
- [49] K. Simonyan and A. Zisserman, "Very deep convolutional networks for large-scale image recognition," *arXiv preprint arXiv:1409.1556*, 2014.